

# Potential of aqueous extract of *Hibiscus sabdariffa* leaves for inhibiting the corrosion of aluminum in alkaline solutions

Ehteram A. Noor

Received: 15 October 2008 / Accepted: 2 February 2009 / Published online: 27 February 2009  
© Springer Science+Business Media B.V. 2009

**Abstract** Chemical (HE and WL) and electrochemical (PDP and EIS) measurements were applied to evaluate the potential of aqueous extract of *Hibiscus sabdariffa* leaves (AEHSL) for inhibiting the corrosion of Al in 0.5 M NaOH. It was found that the inhibition efficiency increases with the increase of AEHSL concentration. Electrochemical measurements revealed that AEHSL acts as a mixed-type inhibitor with inhibition category that belongs to geometric blocking. Adsorption of inhibitor species was found to follow Langmuir and Dubinin–Radushkevich isotherm models and the ability of AEHSL species to be adsorbed physically on the Al surface was illustrated by Dubinin–Radushkevich isotherm parameters. The data obtained from chemical and electrochemical measurements are in reasonably good agreement. Physical adsorption mechanism of AEHSL species on Al surface in 0.5 M NaOH becomes clear cut by following the trend of inhibitor adsorption with solution temperature. Good correlation between AEHSL water-soluble constituents and the suggested physical adsorption mechanism was obtained. Moreover, at a certain concentration of AEHSL ( $1.00 \text{ g L}^{-1}$ ), the Al surface coverage increases with the increase of NaOH concentration up to 0.5 M after which limited decrease was obtained with further increase in NaOH concentration.

**Keywords** Corrosion inhibition · NaOH · Polarization · Impedance · *Hibiscus sabdariffa* · Langmuir · Dubinin–Radushkevich · Physical adsorption

## 1 Introduction

The main properties that make aluminum (Al) a valuable material are its lightweight, strength, recyclability, corrosion resistance, durability, ductility, formability, and conductivity. Due to this unique combination of properties, the variety of applications of aluminum continues to increase. The good corrosion resistance is attributable to a thin oxide film that forms on aluminum upon exposure to the atmosphere or aqueous solutions that protects the metal from further oxidation: unless exposed to some substance or condition that destroys this protective coating, the metal remains protected from corrosion.

The pickling of Al in caustic alkalis for degreasing before anodizing or to give an attractive matter finish is common practice [1, 2]. Alkalis destroy the protective aluminum film very quickly, possibly because  $\text{OH}^-$  ions are positively adsorbed [3] and hence the dissolution rate of aluminum is very high. To inhibit aluminum dissolution in such aggressive solutions, small amounts of corrosion inhibitors can be added to reduce the corrosion rates to acceptable values. In general, corrosion inhibitors incorporate themselves into corrosion product films in such a way as to increase the film's capacity to prevent corrosion. Nowadays, according to the art of green chemistry, the research and development of nontoxic, natural and environmentally friendly inhibitors are carried out in a continuous mode to control the corrosion phenomenon of aluminum in alkaline and/or acidic media [4–11]. However, for 38 years, the use of natural products of plant origin as metallic corrosion inhibitors had been reported by Al-Hosary et al. [12]. They studied the effect of the two main constituents of the aqueous extract of the *Hibiscus sabdariffa* flower (Fig. 1), namely the organic acids and the coloring materials on the dissolution of aluminum and zinc in alkaline solutions. Both constituents were

E. A. Noor (✉)  
Girls' College of Education, Chemistry Department, King  
Abd El-Aziz University, Jeddah, Kingdom of Saudi Arabia  
e-mail: m7o7o7n@hotmail.com



**Fig. 1** The plant of *Hibiscus Sabdariffa*

effective in retarding the dissolution of the two metals, but the activity of the coloring part was considerably higher than that of the organic acids. *Hibiscus subdariffa* (family Malvaceae) is an annual dicotyledonous herbaceous shrub popularly known as ‘karkade’ in Arabic, and ‘Gongura’ in Hindi. In the Ayurvedic literature of India, different parts of this plant have been recommended as a remedy for various ailments such as hypertension, pyrexia, liver disorders, and as an antidote to poisoning chemicals (acid, alkali, pesticides) and venomous mushrooms [13]. A number of active principles from this plant include anthocyanins, flavonols, and protocatechuic acid [14, 15], which have been identified as contributors to the observed medicinal effects of this plant. The objective of this study is to evaluate the potential of aqueous extract of *Hibiscus sabdariffa* leaves, AEHSL (Fig. 1) for inhibiting the corrosion of aluminum in alkaline solutions by chemical (hydrogen evolution, HE, and weight loss, WL) and electrochemical (electrochemical impedance spectroscopy, EIS, and potentiodynamic polarization, PDP) measurements. The effect of temperature on the corrosion rate of aluminum with and without a certain concentration of inhibitor was also investigated, and some thermodynamic parameters for activation process were computed and discussed.

## 2 Experimental procedures

### 2.1 Materials

The extract of *Hibiscus subdariffa* leaves is prepared by heating 20 g of the dried and ground leaves in 250 mL of

de-ionized water for 1 h in a boiling water bath. After filtration, the water was evaporated from the extract in an oven at controlled temperature (50–60 °C) to yield a reddish brown crystalline precipitate (3.92 g). The concentration of the AEHSL was expressed as w/v.

The composition of the commercially pure aluminum used in the present investigation was (wt%): 99.574% Al, 0.002% Cu, 0.003% Zn, 0.100% pb, 0.050% Co, 0.011% Ni, 0.179% Fe and 0.082% Cr. Samples used in both HE and ML measurements were in the form of rods 1 cm in diameter and 5 cm in length. For electrochemical measurements, the Al rod was inserted into a Teflon tube and fixed with an adhesive. The cross-sectional area exposed to the solution was 0.785 cm<sup>2</sup>. Before each experiment, the sample was abraded with emery paper (grade 80–1,000) and washed with de-ionized water, degreased with acetone (CH<sub>3</sub>COCH<sub>3</sub>) and dried with a stream of air. All chemicals were of analytical grade.

### 2.2 Procedures

#### 2.2.1 Chemical measurements

The HE and ML measurements of Al samples in the investigated solutions were determined over a 90-min immersion period as follows:

Fifty milliliters of tested solution (0.5 M NaOH) with and without certain concentration of AEHSL were placed in a vessel basically the same as that described by Mylius [16], and a degreased, weighed Al sample was introduced into the solution. The time was recorded and hydrogen evolved was collected in a 50-mL calibrated tube filled with water. The volume of hydrogen evolved against each recorded time was measured by the downward displacement of water. A plot of hydrogen evolved per unit area against time produced a straight lines of slope represents the corrosion rate (CR<sub>HE</sub>) in mL cm<sup>-2</sup> min<sup>-1</sup>. The system of hydrogen evolution measurements was well illustrated in previous work [17]. At the end of each experiment of HE, the sample was withdrawn from the tested solution, washed thoroughly with de-ionized water followed by acetone, and finally dried with a stream of air and then weighed again. The corrosion rate was calculated in g cm<sup>-2</sup> min<sup>-1</sup> by applying the following equation:

$$CR_{ML} = \frac{m_1 - m_2}{At_{\infty}} \quad (1)$$

where  $m_1$  and  $m_2$  are the mass of Al sample before and after immersion,  $A$  is the surface area and  $t_{\infty}$  is the end time of each experiment. The percentage of inhibition efficiency (IE%) obtained from both HE and ML measurements can be calculated as:

$$IE\% = \left(1 - \frac{CR}{CR^0}\right) \times 100 \tag{2}$$

where CR and CR<sup>0</sup> are the corrosion rates obtained either from HE or ML measurements with and without of certain concentration of AEHSL, respectively.

### 2.2.2 Electrochemical measurements

Electrochemical experiments were conducted through an ACM Gill AC instrument model 655 by using a conventional electrochemical cell of three electrodes with Al as working electrode, Ag/AgCl<sub>(s)</sub>/KCl<sub>saturated (aq)</sub> as the reference electrode, and platinum wire as the auxiliary electrode. The EIS measurements were performed at open circuit potential after 15 min of immersion in the tested solution with amplitude of 10 mV. The covered frequency range was 30 KHz to 0.5 Hz. The charge transfer resistance (*R*<sub>ct</sub>) values were calculated from the difference in the impedance at low and high frequencies. The capacitance of the double layer (*C*<sub>dl</sub>) values is estimated from the frequency (*f*) at which the imaginary component of the impedance (*-Z''*) is maximum and obtained from the equation:

$$f(-Z''_{max}) = \left(\frac{1}{2\pi C_{dl}R_{ct}}\right) \tag{3}$$

The PDP measurements were carried out after the impedance test was completed at a sweep rate of 1 mV/s and within the potential range from -1,700 to -1,300 mV. Tafel lines extrapolation method was used for detecting the electrochemical parameters for the studied systems such as corrosion current density (*i*<sub>corr</sub>) and corrosion potential (*E*<sub>corr</sub>). The percentage inhibition efficiency can be obtained from electrochemical measurements as follows:

$$PDP: IE_i\% = \left(1 - \frac{i_{corr}}{i_{corr}^0}\right) \times 100 \tag{4}$$

where *i*<sub>corr</sub> and *i*<sub>corr</sub><sup>0</sup> are the corrosion current densities with and without of certain concentration of AEHSL, respectively.

$$EIS: IE_R\% = \left(1 - \frac{R_{ct}^0}{R_{ct}}\right) \times 100 \tag{5}$$

where *R*<sub>ct</sub> and *R*<sub>ct</sub><sup>0</sup> are the charge transfer resistance with and without of certain concentration of AEHSL, respectively.

It must be mentioned that all chemical and electrochemical measurements were conducted in open air and we used unstirred solutions at 30 °C unless otherwise stated.

## 3 Results and discussion

### 3.1 Electrochemical measurements

#### 3.1.1 PDP measurements

Figure 2 shows the anodic and cathodic polarization curves for Al in 0.5 M NaOH with and without various concentrations of AEHSL at 30 °C. As can be seen, both cathodic (hydrogen evolution) and anodic (metal dissolution) reactions of Al corrosion were inhibited with the increases of AEHSL in the tested aggressive solution. This result suggests that AEHSL acts as a mixed-type inhibitor. The values of the polarization parameters (*i*<sub>corr</sub>, *E*<sub>corr</sub> and IE<sub>*i*</sub>%) obtained in inhibited and uninhibited alkaline solutions are listed in Table 1. Clearly, *i*<sub>corr</sub> value decreased while IE<sub>PDP</sub>% value increased significantly with an increase in AEHSL concentration. Results also indicated that no definite trend was observed in the shift of *E*<sub>corr</sub> values, in the presence of various concentration of AEHSL.

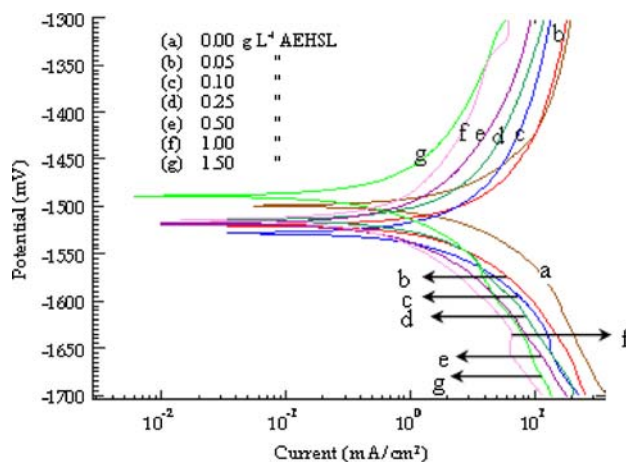


**Fig. 2** Polarization curves of Al in 0.5 M NaOH with and without different concentrations of AEHSL

**Table 1** Corrosion parameters obtained from PDP measurements for Al in 0.5 M NaOH with and without different concentrations of AEHSL

<i>C</i> <sub>inh</sub> (g L <sup>-1</sup> )	<i>-E</i> <sub>corr</sub> (mV)	<i>i</i> <sub>corr</sub> (mA cm <sup>-2</sup> )	IE <sub><i>i</i></sub> %
0.00	1,499.5	2.278	0.00
0.05	1,523.3	1.752	23.09
0.10	1,531.5	1.376	39.60
0.25	1,514.6	0.834	63.38
0.50	1,522.8	0.516	77.35
1.00	1,514.5	0.423	81.43
1.50	1,489.9	0.410	82.00

3.1.2 EIS measurements

The EIS of Al in 0.5 M NaOH with and without various concentrations of AEHSL are summarized as Bode and Nyquist plots in Figs. 3 and 4, respectively. The Bode plots of Fig. 3 of Al clearly show that the addition of an increasing amount of AEHSL led to an increase in the electrode impedance. However, the absence of linear log Z relations with a slope of  $-1$  (especially in the case of an uninhibited system) and the departure of phase angle at intermediate frequencies from  $90^\circ$  shows that the circuit tends to the resistive behavior [18]. The Nyquist plots of Fig. 4 show three parts: the capacitive loop in the high-frequency region, the inductive loop in the middle-frequency region, and the capacitive loop in the low-frequency region. The high-frequency capacitive loop can be attributed to the charge transfer resistance ( $R_{ct}$ ). The inductive loop might have been caused by the adsorbed intermediate (may be  $[AlOH]_{ads}$ ) [19]. The low-frequency

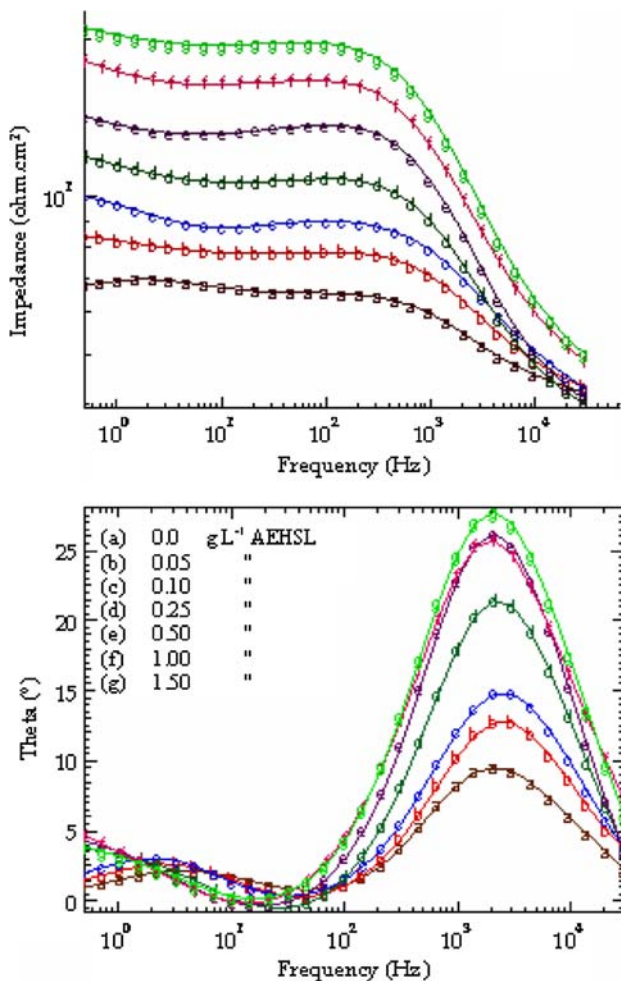


Fig. 3 Bode plots of Al in 0.5 M NaOH with and without different concentrations of AEHSL

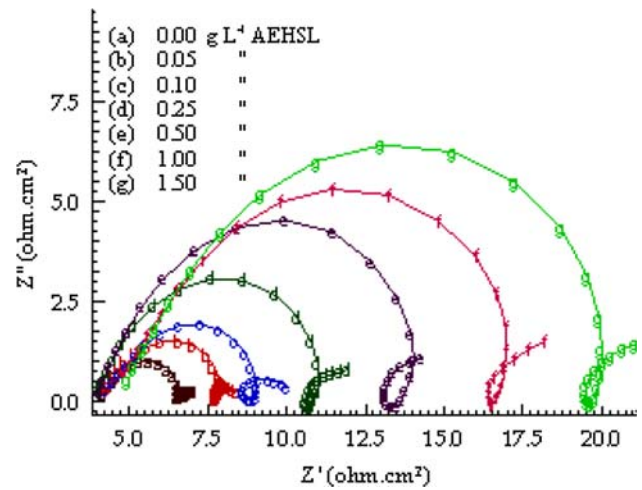


Fig. 4 Nyquist plots of Al in 0.5 M NaOH with and without different concentrations of AEHSL

capacitive loop indicated the growth and dissolution of the surface film [20]. As can be seen in the presence of AEHSL, the Al electrode showed EIS spectra similar to that obtained in the blank solution, only “amplified”, indicating that the inhibition category under this condition belongs to geometric blocking [20, 21].

The equivalent circuit model of the previous systems is shown in Fig. 5. A similar circuit was suggested for the corrosion behavior of the Al electrode in 1.0 M KOH with and without calcium tartrate [20]. Values of  $R_{ct}$ ,  $C_{dl}$  and  $IE_R\%$  for inhibited and uninhibited systems were estimated and are listed in Table 2. Complete inspection of Table 2 reveals that  $R_{ct}$  values increased with increasing inhibitor concentration. On the other hand, the values of  $C_{dl}$  decreased with an increase in AEHSL concentration. This was a result of increasing surface coverage by the inhibitor, which led to an increase in  $IE\%$ . The thickness of the protective layer,  $\delta$ , was related to  $C_{dl}$  by the following equation [22]:

$$\delta = \frac{\epsilon_0 \epsilon_r}{C_{dl}} \tag{6}$$

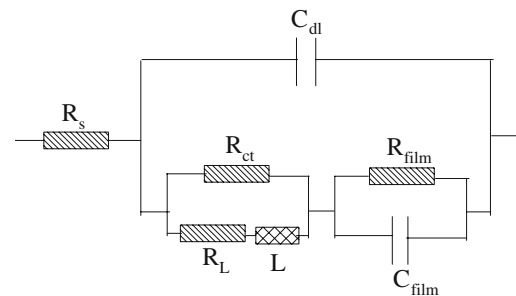


Fig. 5 EIS equivalent circuit of Al in 0.5 M NaOH with and without different concentrations of AEHSL

**Table 2** Corrosion parameters obtained from EIS measurements for Al in 0.5 M NaOH with and without different concentrations of AEHSL

$C_{inh}$ (g L <sup>-1</sup> )	$R_{ct}$ (ohm cm <sup>2</sup> )	$C_{dl}$ (μF cm <sup>-2</sup> )	IE <sub>R</sub> %
0.00	2.374	87.82	0.00
0.05	3.688	59.24	35.63
0.10	4.795	49.41	50.49
0.25	7.287	43.44	67.42
0.50	10.340	27.11	77.04
1.00	13.190	25.12	82.00
1.50	15.500	21.34	84.68

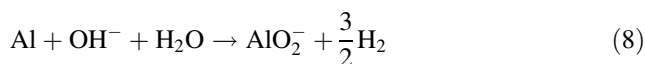
where  $\epsilon_0$  is the vacuum dielectric constant and  $\epsilon_r$  is the relative dielectric constant. So, the decrease in the  $C_{dl}$  value, which can result from a decrease in the local dielectric constant and/or an increase in the thickness of electrode double layer, suggested that the inhibitor species function by adsorption at the metal/solution interface [23, 24].

### 3.2 Chemical measurements

Figure 6 shows the effect of increasing concentrations of AEHSL on the relationship between the volume of hydrogen evolved during the dissolution process per unit area ( $V$ , mL cm<sup>-2</sup>) and the reaction time ( $t$ , min) at 30 °C. It was observed that the hydrogen evolution increases with increasing of immersion time. The variation is linear, which fits the empirical equation:

$$V = CR_{HE}t \tag{7}$$

where  $CR_{HE}$  is the slope ( $dV/dt$ ) and previously defined as the corrosion rate, which depends on additive concentration and solution temperature. It is obvious that the induction period where the alkali seems to react with an oxide film is very short in the blank solution (about 5 min), indicating that the natural oxide (Al<sub>2</sub>O<sub>3</sub>) film that formed on the Al surface is highly soluble in free-inhibitor solutions (0.5 M NaOH) and Al bare surface may corrode by forming soluble species (AlO<sub>2</sub><sup>-</sup>) according [18]:



However, it is obvious from Fig. 6 that the curves of additive containing systems fall below that of the free alkali with induction period varied from 10 min (at 0.05 g L<sup>-1</sup> of inhibitor) to 30 min (at 1.5 g L<sup>-1</sup> of inhibitor). This indicates that AEHSL slow down the rate of hydrogen evolution at all the investigated concentrations may be by incorporating in the natural oxide film leading to the formation of stable or insoluble film, hinder further dissolution. The corrosion rates and inhibition efficiencies

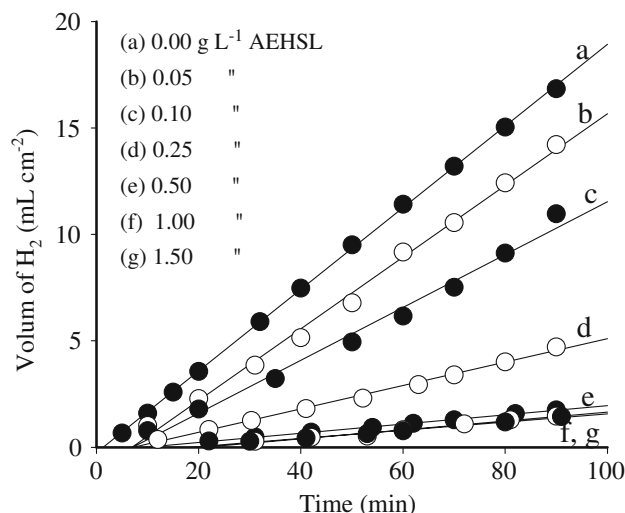


**Fig. 6** Variation of H<sub>2</sub> evolved with time for Al in 0.5 M NaOH with and without different concentrations of AEHSL

values were calculated from both HE and ML measurements and are listed in Table 3. The data revealed that the corrosion rates ( $CR_{HE}$  and  $CR_{ML}$ ) decreased and the corresponding IE% increased with increasing the concentration of AEHSL. So, the addition of an inhibitor retards both the anodic (metal dissolution) and the cathodic (hydrogen evolution) reactions of Al corrosion in the tested solution. However, good consistency between the IE% values obtained from both HE and ML measurements was observed.

### 3.3 Adsorption behavior

Figure 7 illustrates the variations of surface coverage ( $\theta = \frac{IE\%}{100}$ ) obtained from different techniques versus extract concentration. All plots have an S-shaped adsorption isotherm which characterized with the initial increase in the surface coverage with increasing extract concentration up to certain concentration after which the increase in the surface coverage with extract concentration becomes limited, indicating that at a higher level of extract concentration, the metal surface reaches saturation conditions with the adsorbed species.

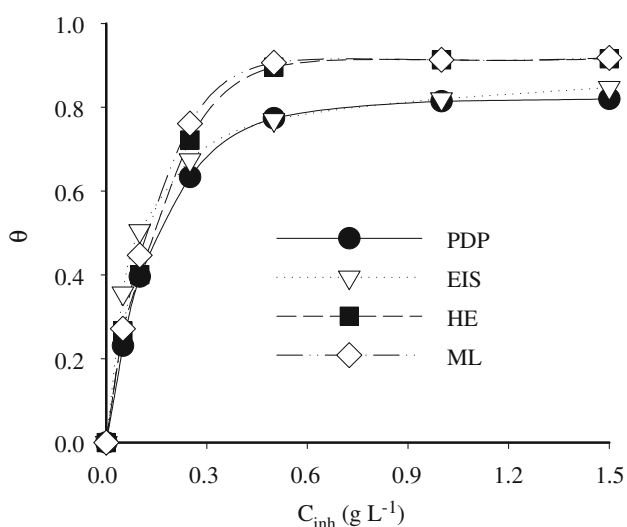
To optimize the design of the above adsorption systems, various isotherm models have been tested to describe the equilibrium characteristics of these systems. It was found that the best description of the adsorption behavior of AEHSL on aluminum in 0.5 M NaOH solutions was obtained by:

#### 3.3.1 Langmuir isotherm model (LIM) [25]

The basic assumption in Langmuir theory is that the adsorption takes place at specific homogeneous sites within

**Table 3** Corrosion parameters obtained from HE and ML measurements for Al in 0.5 M NaOH with and without different concentrations of AEHSL

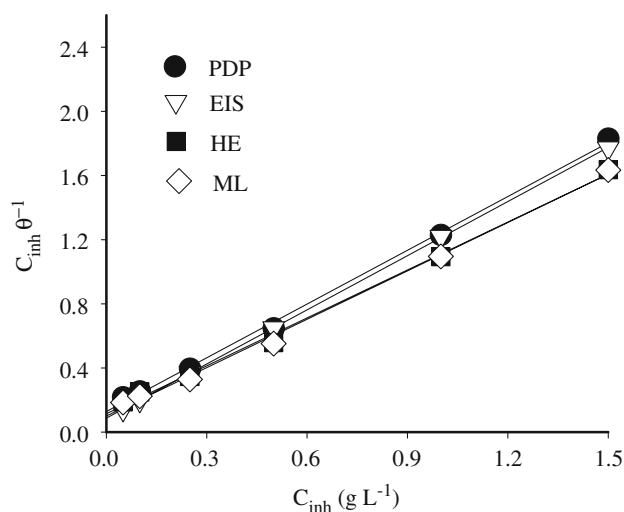
$C_{inh}$ (g L <sup>-1</sup> )	Corrosion rate		Inhibition efficiency	
	$\rho_{HE} \times 10^2$ (mL cm <sup>-2</sup> min <sup>-1</sup> )	$\rho_{ML} \times 10^5$ (g cm <sup>-2</sup> min <sup>-1</sup> )	Inh <sub>HE</sub> %	Inh <sub>ML</sub> %
0.00	18.802	15.219	0.00	0.00
0.05	13.796	11.087	26.62	27.15
0.10	11.177	8.420	40.06	44.67
0.25	5.230	3.634	72.18	76.12
0.50	1.950	1.426	89.63	90.63
1.00	1.625	1.320	91.36	91.33
1.50	1.577	1.246	91.61	91.81

**Fig. 7** Relation between Al surface coverage and concentration of AEHSL

the adsorbent. The Langmuir model is given by the following equation:

$$C_{inh}\theta^{-1} = \frac{1}{K_{ads}} + C_{inh} \quad (9)$$

where  $K_{ads}$  (L  $\times$  g<sup>-1</sup>) is the Langmuir constant, which is defined as the equilibrium adsorption constant. Figure 8 shows the relationship between  $C_{inh}\theta^{-1}$  and  $C_{inh}$  for the obtained data from different techniques. The regression between  $C_{inh}\theta^{-1}$  and  $C_{inh}$  has been done using the computer software SigmaPlot9.0, and the corresponding parameters are listed in Table 4. It was found that all the linear correlation coefficients ( $r^2$ ) and slopes are very close to unity, meaning that the amount of adsorbed species on Al surface increases with the increase of AEHSL concentration up to saturation conditions at which monolayer of adsorbate may be formed.

**Fig. 8** Fitting of the results obtained by different measurements to LIM**Table 4** Langmuir and Dubinin–Radushkevich isotherm parameters obtained from different measurements for AEHSL adsorption on Al surface in 0.5 M NaOH

Adsorption parameters	Electrochemical measurements		Chemical measurements	
	PDP	ML	HE	EIS
<i>LIM</i>				
$r^2$	0.998	1.000	0.996	0.997
Slope	1.12	1.13	0.996	1.01
$K_{ads}$ (L g <sup>-1</sup> )	7.813	11.111	8.772	10.101
$\Delta G_{ads}$ (kJ mol <sup>-1</sup> )	-22.58	-23.47	-22.88	-23.23
<i>D-RIM</i>				
$r^2$	0.996	1.000	0.988	0.988
$\theta_{max}$	0.8869	0.8642	0.9994	0.9851
$a$ (mol <sup>2</sup> kJ <sup>-2</sup> )	0.023	0.015	0.023	0.022
$E$ (kJ mol <sup>-1</sup> )	4.66	5.77	4.66	4.77

$K_{ads}$  value can be related to the free energy of adsorption ( $\Delta G_{ads}$ ) by the following equation:

$$\log K_{ads} = -\log C_{H_2O} - \frac{\Delta G_{ads}}{2.303RT} \quad (10)$$

where  $C_{H_2O}$  is the concentration of water in solution expressed in g L<sup>-1</sup>,  $R$  (kJ mol<sup>-1</sup> K<sup>-1</sup>) is the universal gas constant and  $T$  (K) is the absolute temperature. It must be noted that the concentration unit of water molecules must be similar to that of inhibitor, because there was a common mistake in many corrosion inhibition literatures that used natural products as inhibitors. This was that the used concentration of water is in the molar unit (55.5 M at 25 °C), while the used concentration of inhibitor may express either in mass/volume or volume/volume%, which leads to give uncorrected calculations for  $\Delta G_{ads}$ . In the present

work, this mistake was avoided and the calculated  $\Delta G_{\text{ads}}$  values are listed in Table 4. The negative values of  $\Delta G_{\text{ads}}$  suggests that the adsorption of AEHSL onto the aluminum surface is a spontaneous process. The data in Table 4 revealed good agreement between the results obtained from chemical and electrochemical measurements.

### 3.3.2 Dubinin–Radushkevich isotherm model (D-RIM) [26]

D-RIM was used to distinguish between physical and chemical adsorption for the removal of some pollutants from aqueous solutions by adsorption on various adsorbents [27–30]. It can be expressed as:

$$\ln \theta = \ln \theta_{\text{max}} - a\sigma^2 \tag{11}$$

where  $\theta_{\text{max}}$  is the maximum surface coverage and  $\sigma$  (Polany potential) can be correlated as:

$$\sigma = RT \ln \left( 1 + \frac{1}{C_{\text{inh}}} \right) \tag{12}$$

The constant  $a$  gives the mean adsorption energy,  $E$ , which is the transfer energy of 1 mole of adsorbate from infinity (bulk solution) to the surface of the adsorbent:

$$E = \frac{1}{\sqrt{2a}} \tag{13}$$

The magnitude of  $E$  gives information about the type of adsorption, if this value is less than  $8 \text{ kJ mol}^{-1}$ , adsorption type can be explained by physical adsorption [30]. Figure 9 shows the relationship between  $\ln \theta$  and  $\sigma^2$  for the obtained data from different techniques. The regression between  $\ln \theta$  and  $\sigma^2$  has been done, and the corresponding parameters are listed in Table 4.

$E$  values were estimated from different techniques and are given in Table 4. As can be seen, the numerical values of  $E$  reflect the physical adsorption mechanism. However, the maximum surface coverage ( $\theta_{\text{max}}$ ) obtained from chemical measurements is higher than that obtained from electrochemical measurements. This result may be attributed to the longer immersion period required in the chemical measurements (90 min) at which equilibrium conditions for inhibitor adsorption was expected to be reached successfully. Hence, a monolayer of adsorbate may be completely formed.

### 3.4 Effect of temperature

To gain another insight into the nature of inhibitor adsorption, the effect of temperature (30–60 °C) on the corrosion behavior of Al in 0.5 M NaOH with and without 1.00 g L<sup>-1</sup> of AEHSL was tested by ML measurements. The results revealed that Al corrosion rate in 0.5 M NaOH

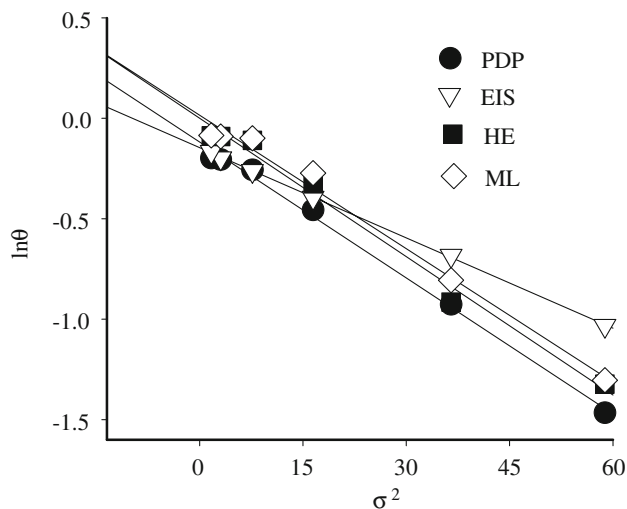


**Fig. 9** Fitting of the results obtained by different measurements to D-RIM

with and without AEHSL increases with temperature increase obeying Arrhenius-type reactions (Fig. 10a) while the corresponding IE% value decreases somewhat with the increase of solution temperature (Fig. 10b).

The apparent activation energy,  $E_{\text{app}}$ , for the corrosion reaction of Al in 0.5 M NaOH with and without 1.00 g L<sup>-1</sup> of AEHSL can be obtained with the help of Arrhenius equation:

$$\log \text{CR} = \log A - \frac{E_{\text{app}}}{2.303RT} \tag{14}$$

where  $A$  is the frequency factor. A plot of  $\log \text{CR}$  versus  $\frac{1}{T}$  gives straight lines (Fig. 11) with slope  $-\frac{E_{\text{app}}}{2.303R}$ . It was found that the values of  $E_{\text{app}}$  for the Al corrosion in 0.5 M NaOH without and with 1.00 g L<sup>-1</sup> AEHSL are 28.33 kJ mol<sup>-1</sup> and 48.69 kJ mol<sup>-1</sup>, respectively. Analysis of the temperature dependence of inhibition efficiency as well as comparison of corrosion activation energies with and without inhibitor gives some insight into the possible mechanism of inhibitor adsorption. Popova et al. [31] reported that a decrease in the inhibition efficiency with a rise in temperature with a corresponding increase in corrosion activation energy in the presence of an inhibitor compared to its absence is frequently interpreted as being suggestive of physical adsorption. For more confirmation, an estimate of the heat of adsorption ( $Q_{\text{ads}}$ ) can be obtained from the trend of surface coverage with temperature as follows [32]:

$$Q_{\text{ads}} = 2.303R \left[ \log \left( \frac{\theta_2}{1 - \theta_2} \right) - \log \left( \frac{\theta_1}{1 - \theta_1} \right) \right] \frac{T_1 T_2}{T_2 - T_1} \tag{15}$$

where  $\theta_1$  and  $\theta_2$  are the surface coverage at temperature  $T_1$  (30 °C + 273) and  $T_2$  (60 °C + 273). It was found that

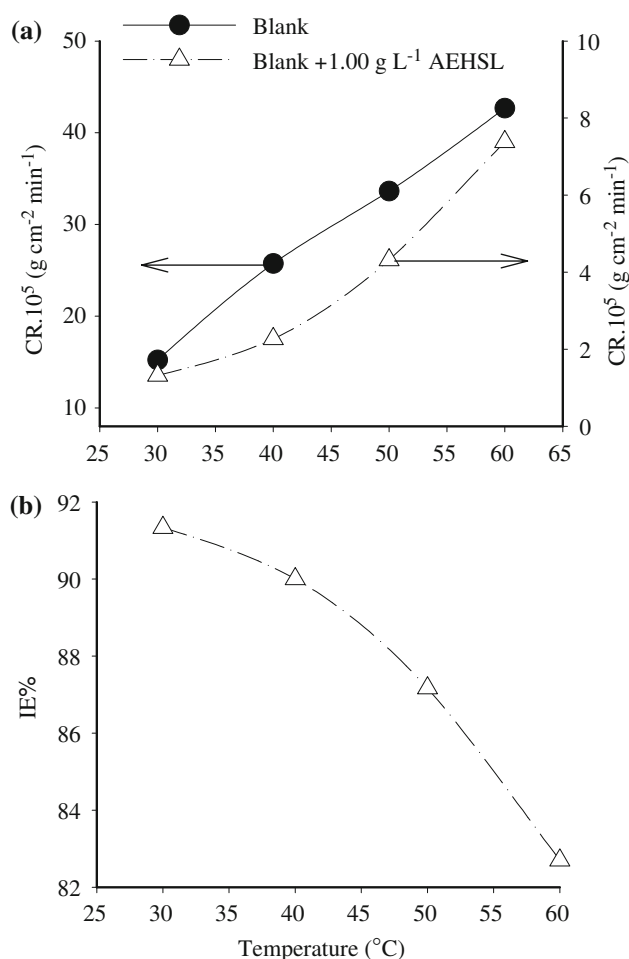


**Fig. 10** Variation of (a) CR and (b) IE% with solution temperature

the adsorption of AEHSL species on the Al surface is an exothermic process associated with a low negative value of adsorption heat ( $Q_{\text{ads}} = -22.09 \text{ kJ mol}^{-1}$ ), so the earlier proposed physical adsorption mechanism is clear cut.

### 3.5 AEHSL constituents and inhibition mechanism

Proximate analysis revealed that per 100 g, the leaf of *Hibiscus subdariffa* contains 85.6% H<sub>2</sub>O, 3.3 g protein, 0.3 g fat, 9.2 g total carbohydrate, 1.6 g fiber, 1.6 g ash, 213 mg Ca, 93 mg P, 4.8 mg Fe, 4.135 mg B-carotene (insoluble in water), 0.17 mg thiamine (soluble in water), 0.45 mg riboflavin (sparingly soluble in water), 1.2 mg niacin (soluble in water) and 54 mg ascorbic acid (soluble in water) [33]. Moreover, in a recent study [34], anthocyanins (soluble in water) were detected in a preliminary analysis of *Hibiscus subdariffa* leaves. Accordingly, it was expected that water-soluble organic constituents (thiamine, niacin, ascorbic acid, and anthocyanins) of *Hibiscus subdariffa* leaves may play an important role in the inhibition mechanism of Al corrosion in the tested solutions. Table 5

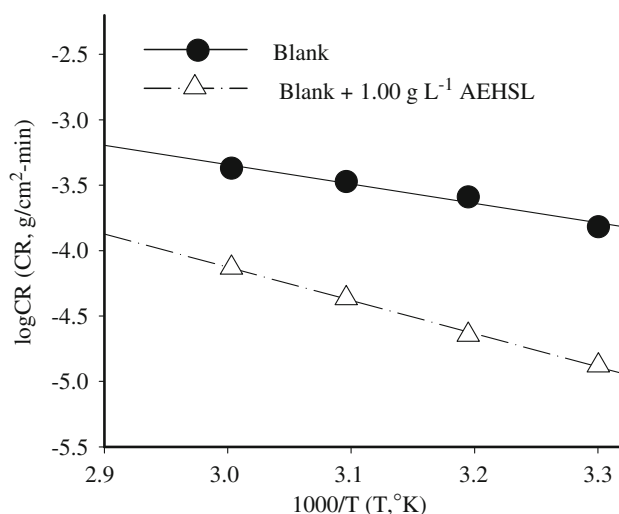


**Fig. 11** Arrhenius plots for Al corrosion in 0.5 M NaOH with and without 1.00 g L<sup>-1</sup> of AEHSL

represents the chemical structure and the bioactivity of these water-soluble constituents [35].

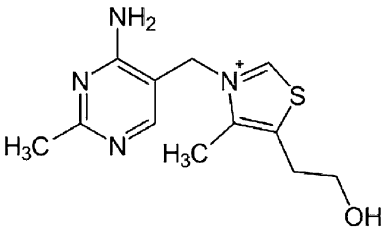
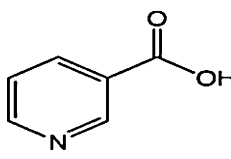
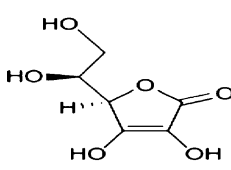
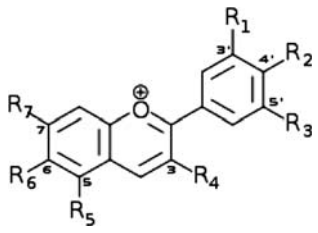
Generally, as the adsorption of organic molecules involves O, N, and S atoms, the organic constituents in Table 5 can be assumed to be effective corrosion inhibitors by blocking active sites and decreasing the corrosion rate. In the present study, a physical adsorption mechanism was suggested to explain the inhibitory action of AEHSL for Al corrosion in 0.5 M NaOH. It is well known that physical adsorption depends on the electric charge of the metal surface and the type of the charged species in solution phase. Two phenomena should be addressed when considering the mechanism of Al dissolution [36]. The first is the development of potentials at the metal–solution interface as a result of composition change in the interfacial region. The second is the presence of a reaction product film (usually oxide). It was reported that the pH of zero charge for aluminum oxide is 9.0–9.1 [37] and during corrosion of aluminum in alkaline solutions ( $\text{pH} > 9.0$ ) the metal establishes very negative potentials [38], so cations are more likely to be adsorbed. Accordingly, the positively charged species in AEHSL (thiamine and anthocyanins) was expected to adsorb under electrostatic attraction with the negatively charged Al surface giving rise to physical adsorption mechanism. However, AEHSL must be handled as a package of inhibitors in which its constituents may act synergistically to inhibit Al corrosion in the tested solutions.

### 3.6 Effect of NaOH concentration

The corrosion rate varies exponentially with the concentration of the aggressive solution by the following equation [39]:



**Table 5** Chemical structure and bioactivity for some of the water soluble constituents of AEHSL

Constituent	Chemical structure	Bioactivity
<p><i>Thiamine</i></p> <p>IUPAC name: 2-[3-[(4-amino-2-methyl-pyrimidin-5-yl)methyl]-4-methyl-thiazol-5-yl] ethanol</p>		<p><i>Thiamine</i>, also known as vitamin B<sub>1</sub>. Thiamine is one of only four nutrients (vitamin B<sub>1</sub>, vitamin B<sub>3</sub>, vitamin C and vitamin D) associated with a pandemic human deficiency disease. It is essential for neural function and carbohydrate metabolism</p>
<p><i>Niacin</i> (Nicotinic acid)</p> <p>IUPAC name: pyridine-3-carboxylic acid</p>		<p><i>Niacin</i>, also known as vitamin B<sub>3</sub>. There are two decisively proven uses of pharmacological doses of niacin. These are for heart disease and skin conditions</p>
<p><i>Ascorbic acid</i></p> <p>IUPAC name: (R)-3,4-dihydroxy-5-((S)-1,2-dihydroxyethyl)furan-2(5H)-one</p>		<p><i>Ascorbic acid</i> is a sugar acid with antioxidant properties. It is water-soluble. The L-enantiomer of ascorbic acid is commonly known as vitamin C. Exposure to oxygen, metals, light, and heat destroys ascorbic acid, so it must be stored in a dark, cold, and non-metallic container</p>
<p><i>Anthocyanins</i></p>		<p><i>Anthocyanins</i> are water-soluble vacuolar pigments. They belong to a parent class of molecules called flavonoids synthesized via the phenylpropanoid pathway. They play an important role as light attenuators and act as powerful antioxidants</p>

$$CR = kC^B \quad (16a)$$

The previous equation can be written in the linear form as follows:

$$\log CR = \log k + B \log C \quad (16b)$$

where  $k$  and  $B$  are the kinetic reaction constants and  $C$  is the concentration of the aggressive medium. Figure 12 represents the relationship between  $\log CR$  obtained from both HE and ML measurements and  $\log C_{\text{NaOH}}$  in absence and presence of certain concentration ( $1.00 \text{ g L}^{-1}$ ) of AEHSL. The kinetic reaction constants ( $k$  and  $B$ ) were estimated and listed in Table 6. The positive values for constant  $B$  indicate that with increasing NaOH concentration, there is systematic increase in the corrosion rate even in the presence of a certain concentration of inhibitor. Anyway, it was found that the inhibited system has  $k$  and  $B$  values lesser than that recorded for the uninhibited system,

indicating that the addition of inhibitor is effectively inhibited by the metal dissolution in the concentration range of aggressive medium.

Figure 13 gives the variation of  $\theta$  with the concentration of NaOH. An interesting behavior is observed that the  $\theta$  value increases with the increase of NaOH concentration up to 0.5 M, then limited decrease was obtained with further increase in NaOH concentration. As previously noted, the aluminum surface is negatively charged in alkaline solutions. So the increase of NaOH concentration enhances the aluminum surface to be more negatively charged, which in turn enhances the physical adsorption of AEHSL species, leading to a modification of the surface coverage, while at a higher level of NaOH concentration ( $>0.5 \text{ M}$ ) the tendency of the metal to react with alkali increases and liberates hydrogen vigorously. This may not allow for the establishment of the adsorption process sufficiently and may result in a decrease of inhibition [40].

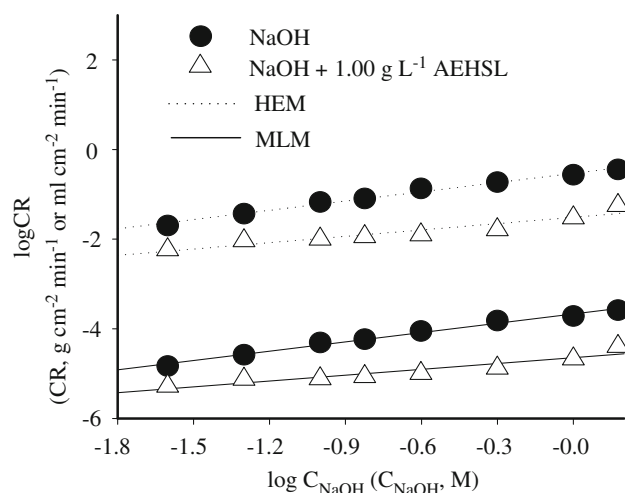


**Fig. 12** Relation between log CR and log  $C_{\text{NaOH}}$  for Al corrosion with and without  $1.00 \text{ g L}^{-1}$  of AEHSL

**Table 6** Kinetic constants obtained from HE and ML measurements for Al corrosion in NaOH solutions with and without  $1.00 \text{ g L}^{-1}$  of AEHSL

The system	$k$		$B$	
	$k_{\text{HE}} \times 10^2$ ( $\text{mL cm}^{-2} \text{ min}^{-1}$ )	$k_{\text{ML}} \times 10^5$ ( $\text{g cm}^{-2} \text{ min}^{-1}$ )	HE	ML
NaOH	29.580	21.380	0.689	0.691
NaOH + $1.00 \text{ g L}^{-1}$ AEHSL	3.083	2.259	0.476	0.434

#### 4 Conclusions

- AEHSL was found to be an effective inhibitor for the corrosion of Al in an alkaline solution. The inhibition efficiency increases with the increase of AEHSL concentration.
- Electrochemical measurements revealed that AEHSL acts as mixed-type inhibitor with inhibition category belonging to geometric blocking.
- Adsorption of inhibitor species was found to follow *Langmuir* and *Dubinina–Radushkevich* isotherm models and the ability of AEHSL species to adsorbed physically on Al surface was illustrated by *Dubinina–Radushkevich* isotherm parameters.
- The data obtained from HE, WL, PDP, and EIS measurements are in reasonably good agreement.
- The inhibition efficiency of AEHSL is temperature-dependent, and its addition leads to a relative increase of apparent activation corrosion energy.
- Physical adsorption mechanism of AEHSL species on Al surface in  $0.5 \text{ M}$  NaOH becomes clear cut by following the trend of inhibitor adsorption with solution temperature.

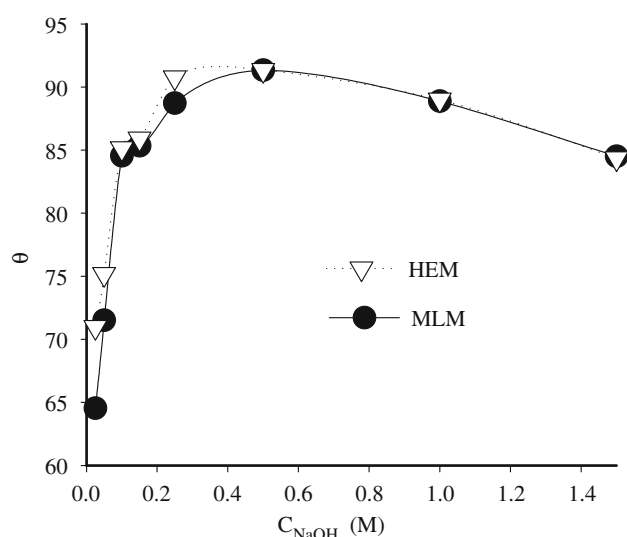


**Fig. 13** Relation between Al surface coverage and concentration of NaOH

- Good correlation between AEHSL water-soluble constituents and the suggested physical adsorption mechanism was obtained.
- At certain a concentration of AEHSL ( $1.00 \text{ g L}^{-1}$ ), the Al surface coverage with inhibitor species increases with the increase of NaOH concentration up to  $0.5 \text{ M}$ , after which limited decrease was obtained with further increase in NaOH concentration.

#### References

1. Putilova IN, Barannik VP, Balezin SA (1960) Metallic corrosion inhibitors. Pergamon Press, Oxford, p 124
2. Burns RM, Bradley WW (1967) Protective coating for metals. Reinhold, New York, p 29
3. Evans UR (1983) An introduction to metallic corrosion. Edward Arnold, London, p 69
4. El-Etre AY (2001) Inhibition of acid corrosion of aluminium using vanillin. *Corros Sci* 43:1031–1039
5. El-Etre AY (2003) Inhibition of aluminium corrosion using *Opuntia* extract. *Corros Sci* 45:2485–2495
6. Avwiri GO, Igho FO (2003) Inhibitive action of *Vernonia amagdalena* on the corrosion of aluminium alloys in acidic media. *Mater Lett* 57:3705–3711
7. El-Etre AY, Abdallah M, El-Tantawy ZE (2005) Corrosion inhibition of some metals using *Lawsonia* extract. *Corros Sci* 47:385–395
8. Umoren SA, Obot IB, Ebenso EE, Okafor PC, Ogbobe O, Oguzie EE (2006) Gum arabic as a potential corrosion inhibitor for aluminium in alkaline medium and its adsorption characteristics. *Anti-Corros Meth Mater* 53/5:277–282
9. Oguzie EE (2007) Corrosion inhibition of aluminium in acidic and alkaline media by *Sansevieria trifasciata* extract. *Corros Sci* 49:1527–1539
10. Arora P, Humar S, Sharma MK, Mathur SP (2007) Corrosion inhibition of aluminium by *Capparis decidua* in acidic media. *E-J. Chem.* 4/4:450–456
11. Arab ST, Al-Turkustani AM, Al-Dhahiri RH (2008) *J Kor Chem Soc* 52/3:281–294

12. Al-Hosary AA, Saleh RM, Sams El-Din AM (1972) Corrosion inhibition by naturally occurring substances-I. The effect of *Hibiscus subdariffa* (Karkade) extract on the dissolution of Al and Zn. *Corros Sci* 12:897–904
13. Essa MM, Subramanian P, Mnivasagam T, Dakshayani KB, Sivaperumal R, Subash S (2006) Protective influence of *Hibiscus sabdariffa* an edible medicinal plant, on tissue lipid peroxidation and antioxidant status in hyperammonemic rats. *Afr J Tradit Complement Altern Med* 3/3:10–21
14. Osman AM, Al-Garby Younes M, Mokhtar A (1975) Sitosterol—galactoside from *Hibiscus sabdariffa*. *Phytochemistry* 14/3:829–830
15. Seca AML, Silva AMS, Silvestre AJD, Cavaleiro JAS, Domingues FMJ, Neto CP (2001) Phenolic constituents from the core of kenaf (*Hibiscus cannabinus*). *Phytochemistry* 56:759–767
16. Mylius FZ (1922) *Metalkade* 14:233
17. Noor EA, Al-Moubaraki A (2008) Corrosion behaviour and mechanism for mild steel in hydrochloric acid solutions. *Int J Electrochem Sci* 3:806–813
18. Mazhar AA, Arab ST, Noor EA (2001) Electrochemical behaviour of Al–Si alloy in acid and alkaline media. *Bull Electrochem* 17/10:449–458
19. Paramasivam M, Surech G, Muthuramalingam B, Iyer SV, Kapali V (1991) Different commercial grades of aluminium as galvanic anodes in alkaline zincate solutions. *J Appl Electrochem* 21/5:452–456
20. Shao HB, Wang JM, Zhang Z, Zhang JQ, Cao CN (2001) Inhibition effect of calcium tartrate on the corrosion of pure aluminium in alkaline solutions. *Corrosion (NACE)* 57/7:577–581
21. Cao C (1996) On electrochemical techniques for interface inhibitor research. *Corros Sci* 38/12:2073–2082
22. Dean JA (1973) *Lange's handbook of chemistry*, 2nd edn. McGraw-Hill, New York, p 148.E
23. McCafferty E, Hackerman N (1972) Double layer capacitance of iron and corrosion inhibition with polymethylene diamines. *J Electrochem Soc* 119:146–154
24. Bentiss F, Lagrenee M, Elmehdi B, Mernari B, Traisnel M, Vezin H (2002) Electrochemical and quantum chemical studies of 3, 5-di(n-Tolyl)-4-Amino-1, 2,4-triazole adsorption on mild steel in acidic media. *Corrosion (NACE)* 58/5:399–407
25. Langmuir I (1917) The constitution and fundamental properties of solid and liquids. II. Liquids. *J Am Chem Soc* 39:1848–1906
26. Dubinin MM, Radushkevich LV (1947) *Proc Acad Sci USSR Phys Chem Soc* 55:331
27. Gemeay AH, El-Sherbiny AS, Zaki AB (2002) Adsorption and kinetics studies of the intercalation of some organic compounds onto Na<sup>+</sup>-montmorillonite. *J Colloid Interface Sci* 245:116–125
28. Gemeay AH (2002) Adsorption characteristics and the kinetics of the cation exchange of rhodamine-6G with Na<sup>+</sup>-montmorillonite. *J Colloid Interface Sci* 251:235–241
29. Mall ID, Srivastava VC, Agrawal NK, Mishra IM (2005) Adsorptive removal of malachite green dye from aqueous solutions by bagasse fly ash and activated carbon-kinetic study and equilibrium isotherm analysis. *Colloids Surf A Physicochem Eng Asp* 264:17–28
30. Karahan S, Yurdakoc M, Seki Y, Yurdakoc K (2006) Removal of boron from aqueous solution by clays and modified clays. *J Colloid Interface Sci* 293/1:36–42
31. Popova A, Sokolova E, Raicheva S, Christov M (2003) AC and DC study of the temperature effect on mild steel corrosion in acid media in the presence of benzimidazole derivatives. *Corros Sci* 45/1:33–58
32. Noor EA (2008) Electrochemical study for the corrosion inhibition of mild steel in hydrochloric acid by untreated and treated camel's urine. *Eur J Sci Res (EJSR)* 20/3:496–507
33. Hanson AA, Christie BR (1987) *Handbook of plant science in agriculture*. CRC Press, Boca Raton
34. Morris JB, Wang ML (2007) Anthocyanin content in leaves and flowers of several *Hibiscus* species. In: Association for the advancement of industrial crops conference, p 45
35. <http://en.wikipedia.org/wiki/Thiamine>,  
<http://en.wikipedia.org/wiki/Niacin>,  
[http://en.wikipedia.org/wiki/Ascorbic\\_acid](http://en.wikipedia.org/wiki/Ascorbic_acid),  
<http://en.wikipedia.org/wiki/Anthocyanins>
36. Foley RT, Trzaskoma PP (1977) The chemical nature of the anion dependency of the corrosion of aluminium alloy 7075-T6. *Corrosion (NACE)* 33/12:435–441
37. Tschapek M, Wasowski C, Torres Sanchez RM (1976) The p.z.c. and i.e.p. of  $\gamma$ -Al<sub>2</sub>O<sub>3</sub> and TiO<sub>2</sub>. *J Electroanal Chem* 74:167
38. Cooper JF (1979) Weight and volume estimates for aluminium-air batteries designed for electric vehicle application. In: Proceedings of first international workshop on reactive metal-air batteries, University of Bonn, Bonn, Germany, p 81
39. Mathur PB, Vasudevan T (1982) Reaction rate studies for the corrosion of metals in acids-I, iron in mineral acids. *Corrosion (NACE)* 38/3:171–178
40. Talati JD, Gandhi DK (1983) N-heterocyclic compounds as corrosion inhibitors for aluminium–copper alloy in hydrochloric acid. *Corros Sci* 23/1:1315–1332